Differentiation of Mouse Embryonic Stem Cells Toward Functional Pancreatic β-Cell Surrogates Through Epigenetic Regulation of *Pdx1* by Nitric Oxide

Carmen Salguero-Aranda,*†‡§ Rafael Tapia-Limonchi,*¶[1] Gladys Margot Cahuana,*¶ Ana Belen Hitos,*†
Irene Diaz,*† Abdelkrim Hmadcha,*‡§ Mario Fraga,# Franz Martín,*†¶ Bernat Soria,*†‡§
Juan Rigoberto Tejedo,*†‡¶ and Francisco Javier Bedoya*†‡¶

*Andalusian Center for Molecular Biology and Regenerative Medicine, Seville, Spain
†Center for Network Research in Diabetes and Metabolic Diseases (CIBERDEM) Instituto de Salud Carlos III, Madrid, Spain
‡Cell Therapy Network, Madrid (RED-TERCEL), Instituto de Salud Carlos III, Madrid, Spain
§Fundación Progreso y Salud, Seville, Spain
¶Pablo de Olavide University, Seville, Spain
#Department of Epigenetics, Oncologic Institute of Principado de Asturias, Oviedo, Spain

Pancreatic and duodenal homeobox 1 (Pdx1) is a transcription factor that regulates the embryonic development of the pancreas and the differentiation toward β cells. Previously, we have shown that exposure of mouse embryonic stem cells (mESCs) to high concentrations of diethylenetriamine nitric oxide adduct (DETA-NO) triggers differentiation events and promotes the expression of *Pdx1*. Here we report evidence that *Pdx1* expression is associated with release of polycomb repressive complex 2 (PRC2) and P300 from its promoter region. These events are accompanied by epigenetic changes in bivalent markers of histones trimethylated histone H3 lysine 27 (H3K27me3) and H3K4me3, site-specific changes in DNA methylation, and no change in H3 acetylation. On the basis of these findings, we developed a protocol to differentiate mESCs toward insulin-producing cells consisting of sequential exposure to DETA-NO, valproic acid, and P300 inhibitor (C646) to enhance Pdx1 expression and a final maturation step of culture in suspension to form cell aggregates. This small molecule-based protocol succeeds in obtaining cells that express pancreatic β-cell markers such as PDX1, INS1, GCK, and GLUT2 and respond in vitro to high glucose and KCl.

Key words: Embryonic stem cells (ESCs); Nitric oxide (NO); Cell differentiation;
Insulin-producing cells; Diabetes

INTRODUCTION

Research efforts have been made over the last 15 years to generate pancreatic β-cell surrogates from stem cells. Thus, generation of definitive endoderm from embryonic stem cells (ESCs) and subsequent differentiation into pancreatic progenitors and glucose-responsive pancreatic β cells have been reported[1–8]. The biology of pancreas development might be instrumental in providing information to optimize current differentiation protocols. In this regard, the transcription factor pancreatic and duodenal homeobox 1 (Pdx1) stands out as a relevant regulator of pancreatic development and differentiation toward β cells[9,10]. *Pdx1* gene expression is controlled by the interaction of a set of transcription factors with highly conserved sequences of its promoter[11]. Additional regulatory mechanisms such as DNA methylation and histone covalent modifications have been reported to be relevant in the repression of *Pdx1* in a model of type 2 diabetes[12].

On the other hand, polycomb repressive complex 2 (PRC2) plays a role in the regulation of key developmental genes in ESCs[13,14]. PRC2 catalyzes di- and trimethylation of histone H3 Lys 27 residue (H3K27me2/3), which has been associated with the silencing of target genes[13–16]. PRC2 recruitment to target genes is dependent on jumonji, AT rich interactive domain 2 (JARID-2), whose expression is regulated by stemness factors octamer-binding transcription factor 4 (OCT-4), (sex-determining region Y)-box 2 (SOX2), and NANOG[17–22]. Indeed, PRC2 activity represses *Pdx1* gene expression[17], and epigenetic changes of the *Pdx1* gene have been reported in ESCs during generation of pancreatic endoderm (PE)[23]. On the other hand, persistence of both acetyl-histone H3 (AcH3) and trimethylated histone

H3 lysine 27 (H3K27me3) marks on the silent *Pdx1* gene in hepatoblasts has been reported[24]. In addition, histone acetyltransferase P300 activity has been reported to be involved in the selection of liver over pancreas fate[24]. P300 also acts as a repressor independently of its acetyltransferase activity, since sumoylation of cell cycle regulatory domain 1 (CRD1), a repressor domain of P300, induces the recruitment of histone deacetylase 6 (HDAC6) to promoters susceptible to P300-mediated repression such as *p21* and *survivin*[25,26].

Nitric oxide (NO) is a regulator of stem cell fate, and successful generation of definitive endoderm from ESCs has been achieved by exposure to chemical NO donors in a differentiation protocol with transient expression of *Pdx1* during the process[6,27]. In the present study, we sought to explore the mechanisms involved in the regulation of *Pdx1* by NO and found that this action entails the release of PRC2 and P300 from its promoter region. These events are accompanied by changes in bivalent marks of histone H3K27me3 and H3K4me3 and in the methylation status of specific CpG islands. Given the role of P300 in the regulation of *Pdx1,* we optimized a differentiation protocol for generating insulin-producing cells from ESCs by the addition of P300 inhibitor C646 (P300i) followed by culture in suspension. This protocol succeeds in obtaining cell clusters with sustained expression of pancreatic β-cell markers such as *Pdx1*, insulin-1 (*Ins1),* glucokinase (*Gck), Kir6.2*, and glucose transporter, member 2 (*Glut2)* and that are responsive to conventional secretagogues such as glucose and KCl.

MATERIALS AND METHODS

Cell Culture and Treatments

Mouse ESC (mESC) lines D3 and R1/E [American Type Culture Collection (ATCC), Manassas, VA, USA] were used. INS-1E cells were provided by Dr. P. Maechler (Geneva University, Geneva, Switzerland). D3 and R1/E mESCs were maintained in feeder free culture at 37°C with 5% CO_2 in Dulbecco's modified Eagle's medium (DMEM) (Gibco, Grand Island, NY, USA), supplemented with 15% fetal bovine serum (FBS) (Hyclone, Logan, UT, USA), 0.1 mM β-mercaptoethanol (Gibco, Paisley, Scotland, UK), 2 mM L-glutamine (Gibco, Paisley, Scotland, UK), 1% minimum essential medium (MEM) nonessential amino acids (Gibco, Paisley, Scotland, UK), and 100 U/ml penicillin:100 µg/ml streptomycin (Gibco, Paisley, Scotland, UK). The undifferentiated state was maintained by addition of leukemia inhibitory factor (LIF) (1,000 U/ml) (ESGRO, Chemicon, Charlottesville, VA, USA). INS-1E cells were cultured in Roswell Park Memorial Institute (RPMI)-1640 medium (Lonza, Verviers, Belgium), supplemented with 10% FBS, 10 mM *N*-2-hydroxyethylpiperazine-*N*-2-ethane sulfonic acid (HEPES; Gibco, Paisley, Scotland, UK), 1 mM

sodium pyruvate (Gibco, Paisley, Scotland, UK), 100 U/ml penicillin:100 µg/ml streptomycin, 2 mM L-glutamine, and 50 µM β-mercaptoethanol (Gibco, Paisley, Scotland, UK). R1/E cells, which were used to study the *Pdx1* gene regulation, were cultured for 3 days in gelatinized dishes in the presence or absence of LIF and then exposed to 500 µM diethylenetriamine nitric oxide adduct (DETA-NO) (Sigma-Aldrich, St. Louis, MO, USA) for 19 h. Cultured cells were then disaggregated with trypsin solution (Gibco, Paisley, Scotland, UK) and collected by centrifugation at $230 \times g$. For differentiation protocols, D3 cells were cultured for 3 days without LIF, 19 h with 500 µM DETA-NO, 6 days with 100 µM valproic acid (Sigma-Aldrich), and 20 h with 50 µM P300 inhibitor C646 (Millipore, Darmstadt, Germany). Cell aggregates were then gently scraped and transferred to Falcon tubes (Thermo Fisher Scientific, Waltham, MA, USA) and allowed to sediment for 10 min. The resulting aggregates were then grown in suspension in 12- to 24-well plates for 3 days. On the fifth day of culture, FBS was reduced to 2% until the end of the protocol. Culture medium was changed daily.

RNA Isolation, Reverse Transcription PCR, and Real-Time PCR Analysis

Total RNA was extracted using Easy Blue reagent (Intron Biotechnology, Gyeonggi-do, South Korea) and chloroform/isopropanol purification procedure. cDNA synthesis was performed with 1 µg of total RNA using Moloney murine leukemia virus (M-MVL) reverse transcriptase (Promega, Madison, WI, USA) and random primers according to the manufacturer's instructions. Genes were analyzed by qualitative polymerase chain reaction (PCR). Primer melting temperature (T_m) for all genes was designed at 60°C using MyTaq Red DNA polymerase (Bioline Reagents Ltd, London, UK) with the following specifications: amplification for 35–40 cycles of denaturation at 95°C for 30 s, annealing at 60°C for 15 s and extension at 72°C for 30 s, and a final extension at 72°C for 10 min. PCR was performed in a MyCycler (Bio-Rad Laboratories, Hercules, CA, USA) thermal cycler. For real-time PCR (RT-PCR) analysis, endogenous mRNA levels were measured based on SYBR Green (Applied Biosystems, Foster City, CA, USA) detection with the ABI Prism 7500 machine (Applied Biosystems). Results were normalized with *β-actin* expression. PCR primers used are shown in Supplementary Table 1 (available at http://www.cabimer.es/web/docs/grupos/tcmr2/Material SuplementarioCellTrasplantation.zip).

Western Blotting

Cells were trypsinized, centrifuged at $230 \times g$, and washed once with cold phosphate-buffered saline (PBS) (Gibco, Paisley, Scotland, UK). Cell pellets were then resuspended and incubated in radioimmunoprecipitation

assay (RIPA) buffer (Sigma-Aldrich) supplemented with protease inhibitors (Sigma-Aldrich) and phosphatase inhibitor cocktail (Sigma-Aldrich) for 45 min on ice and sonicated with four pulses (10 s each) at 10% amplitude in a Branson sonifier (Branson Ultrasonics Corporation, Danbury, CT, USA). After centrifugation at $9,300 \times g$, protein content in supernatants were quantified by Bradford assay. Proteins were denatured in Laemmli buffer containing 62.5 mM Tris-HCl (pH 6.8), 2% sodium dodecyl sulfate (SDS), 10% glycerol, 0.01% bromophenol blue, and 2.5 % β-mercaptoethanol (all Sigma-Aldrich) for 10 min at 96°C. Proteins were separated by SDS polyacrylamide gel electrophoresis (SDS-PAGE) and transferred to polyvinylidene difluoride (PVDF) membranes (GE Healthcare, Buckinghamshire, UK). Membranes were then blocked with Tris-buffered saline (Sigma-Aldrich) supplemented with 0.1% Tween 20 (TBST; Sigma-Aldrich) containing 5% skim milk (Becton Dickinson, Franklin Lakes, NJ, USA) for 1 h at room temperature (RT). Then membranes were probed with anti-Pdx1 (1:2,000; Abcam, Cambridge, UK), anti-P300 (1:1,000; Santa Cruz Biotechnology, Heidelberg, Germany), anti-Jarid-2 (1:1,000; Abcam), anti-Ezh2 (1:500; BD Biosciences, San Jose, CA, USA), and anti-β-actin (1:10,000; Sigma-Aldrich) in TBST with 5% skim milk overnight at 4°C. Membranes were subsequently washed three times with TBST. Secondary antibodies used were anti-rabbit immunoglobulin G (IgG) (1:20,000, Sigma-Aldrich) and anti-mouse IgG (1:40,000; Jackson ImmunoResearch, Suffolk, UK). Proteins were detected by chemiluminescence with WesternBright ECL HRP substrate (Advansta Inc., Menlo Park, CA, USA).

Immunocytochemistry

R1/E cells (1.5×10^4) were cultured in wells containing Permanox slides (Thermo Fisher Scientific) and maintained at 37°C with 5% CO_2. To analyze PDX1 expression, cells exposed to DETA-NO for 19 h were fixed with 4% paraformaldehyde (PFA) (Panreac AppliChem, Barcelona, Spain), permeabilized with cold methanol, and blocked with 4% bovine serum albumin (BSA) (Sigma-Aldrich). Cells were incubated overnight with anti-Pdx1 (1:100; Abcam) and anti-α-tubulin (1:300; Sigma-Aldrich). For immunofluorescence of islet-like clusters (D3 cells), clusters were fixed with 4% PFA in PBS overnight at 4°C, dehydrated with ethanol and xylene, and embedded in paraffin (Merk, Darmstadt, Germany). Sections were cut at a thickness of 5 μm with a Leica DM6000B microtome (Leica Microsystems Inc., Concord, ON, Canada). Sections were deparaffinized through a series of xylene and ethanol washes, incubated in PBS for 5 min, and the samples were autoclaved with a 0.01 M citrate buffer (Sigma-Aldrich) for antigen retrieval. Sections were blocked with 3% BSA and 0.2% Triton X-100 (Sigma-Aldrich) in PBS

for 1 h at RT and incubated overnight at 4°C with anti-Pdx1 (1:100; Developmental Studies Hybridoma Bank, Iowa City, IA, USA), anti-C-peptide (1:100; Beta Cell Biology, Vanderbilt University, Nashville, TN, USA), and anti-Glut2 (1:100; Chemicon). Finally, cells were washed three times with PBS and 0.1% Tween (PBST), and detection of primary antibodies was carried out using anti-rabbit Alexa Fluor 594 (1:300; Invitrogen, Carlsbad, CA, USA) and anti-mouse Alexa Fluor 488 (1:300, Invitrogen). 4′,6-Diamidino-2-phenylindole (DAPI) (Sigma-Aldrich) counterstaining was also performed. Fluorescent images were visualized with a Leica DM 5500 microscope (Leica Microsystems, Wetzlar, Germany). Images were processed with Adobe Photoshop (Adobe Systems Incorporated, San Jose, CA, USA).

Flow Cytometry

Cultured cells were detached by trypsinization and collected following centrifugation at $230 \times g$. Cell pellets were fixed with 4% PFA for 10 min at RT, permeabilized with 0.5% Triton X-100 for 10 min on ice, and blocked with PBS 5% FBS at 4°C for 30 min. Cells were then incubated at 4°C for 1 h with anti-Pdx1 (1:600; Abcam) or anti-rabbit IgG-phycoerythrin (PE) goat isotype control (1:600; Abcam) in PBS 5% FBS. Cells were washed three times at 4°C with PBS and exposed to the secondary antibody, anti-rabbit IgG-PE (1:500; Abcam), for 30 min at RT. After three washes with PBS, cells were resuspended in 500 μl of PBS, and fluorescence readouts were carried out by flow cytometry (BD FACSCalibur; BD Biosciences).

Bisulfite Sequencing PCR (BSP)

A region of approximately 2,000 base pairs (bp) of the *Pdx1* promoter was analyzed with the software Methyl Primer Express v1.0. (Applied Biosystems) to identify CpG-rich islands. Primers designed for these regions are listed in Supplementary Table 1 (available at http://www.cabimer.es/web/docs/grupos/tcmr2/Material SuplementarioCellTrasplantation.zip). Then genomic DNA from 7.5×10^4 cells was converted with sodium bisulphite using the Cells-to-CpG Bisulfite Conversion Kit (Applied Biosystems). Converted DNA was amplified by PCR using MyTaq HS Red DNA Polymerase (Bioline Reagents), and then PCR products were purified and cloned into pGEM-T to obtain *Escherichia coli* (*E. coli)* colonies. Ten colonies per treatment were analyzed by PCR and later sequenced in a DNA analyzer 3730 (Applied Biosystems). The results were analyzed by the BiQ Analyzer Software (Max-Planck-Institute and Saarland University, Saarbrücken, Germany).

Bisulfite Pyrosequencing

The results obtained by BSP were confirmed by pyrosequencing. Sodium bisulphite modification of genomic DNA of 7.5×10^4 cells was carried out as described above.

Converted DNA was eluted in 15 µl, and 2 µl was used for each PCR cycle. Primers used for PCR and sequencing were designed using PyroMark assay design software, version 2.0.01.15 (Qiagen, Hilden, Germany). Pyrosequencing primers are shown in Supplementary Table 1 (available at http://www.cabimer.es/web/docs/grupos/tcmr2/Material SuplementarioCellTrasplantation.zip). These primers were designed to hybridize with CpG-free sites to ensure methylation-independent amplification. PCR was performed with biotinylated primers to convert the PCR product to single-stranded DNA templates using the Vacuum Prep Tool (Biotage, Uppsala, Sweden) according to the manufacturer's instructions. Pyrosequencing reactions and methylation quantification were performed in a PyroMark Q24 System version 2.0.6 (Qiagen).

Chromatin Immunoprecipitation Assay (ChIP)

Cells were cross-linked with 1% (w/v) formaldehyde (Sigma-Aldrich) for 10 min at 37°C. Cells (3×10^6) were resuspended in lysis buffer containing 10 mM NaCl, 10 mM Tris-HCl (pH 8), 3 mM Cl$_2$Mg, and 0.5 mM DTT supplemented with protease inhibitors (Sigma-Aldrich) for 10 min on ice. Cells were then centrifuged for 5 min at $800 \times g$ at 4°C. Supernatants were discarded, and the nuclei-containing fraction was washed by gentle inversion with buffer containing 10 mM Tris-HCl (pH 8), 15 mM NaCl, and 60 mM KCl (Sigma-Aldrich). Cell nuclei were subsequently centrifuged for 5 min at $800 \times g$ at 4°C and incubated with washing buffer supplemented with 3 mM CaCl$_2$, protease inhibitors, 0.5 mM 1,4-dithiothreitol (DTT; Sigma-Aldrich), and 5–10 µl of micrococcal nuclease (1:200 dilution) (New England BioLabs, Ipswich, MA, USA). Cell nuclei were incubated for 20 min at 37°C with orbital shaking. Nuclease activity was halted by the addition of 20 µl of 0.5 mM ethylenediaminetetraacetic acid (EDTA; Sigma-Aldrich). Cell nuclei were centrifuged for 5 min at $800 \times g$ at 4°C and lysed with buffer containing 150 mM NaCl, 50 mM Tris-HCl (pH 7.5), 5 mM EDTA, 0.5% NP-40, 1% Triton, and 0.01% SDS and sonicated with three pulses for 10 s each at 10% amplitude in a Branson sonifier. Extracts were then centrifuged for 10 min at $9,300 \times g$ at 4°C. Supernatants containing chromatin with an average size of 500 bp were immunoprecipitated with anti-P300 (4 µg; Santa Cruz Biotechnology), anti-Jarid-2 (3 µg; Abcam), anti-acetylated H3 (1 µg; Abcam), anti-H3K4me3 (1 µg; Abcam), and anti-H3K27me3 (1 µg; Cell Signaling Technology Inc.; Danvers, MA, USA). Rabbit control IgG (Abcam) and mouse IgG1 isotype control mAb (Cell Signaling Technology Inc.) were used as ChIP controls. Dynabeads (15 µl; Invitrogen Dynal AS, Oslo, Norway) was used to prepare Ab–bead complexes and incubated for 30 min at 4°C under rotation in dilution buffer [0.01% SDS, 1.1% Triton X-100, 1.2 mM EDTA, 16.7 mM Tris-HCl (pH 8.1), 167 mM NaCl]. Then chromatin was added and incubated for 1 h. Washes of the complex were once with low-salt buffer [0.1% SDS, 1% Triton X-100, 2 mM EDTA, 20 mM Tris-HCl (pH 8.1), 150 mM NaCl], once with high-salt buffer [0.1% SDS, 1% Triton X-100, 2 mM EDTA, 20 mM Tris-HCl (pH 8.1), 500 mM NaCl], once with LiCl buffer [0.25 M LiCl (Sigma-Aldrich), 1% Igepal CA-630 (Sigma-Aldrich), 1% deoxycholate (Sigma-Aldrich), 1 mM EDTA, 10 mM Tris-HCl (pH 8)], twice with TE buffer [10 mM Tris-HCl (pH 8.1), 1 mM EDTA], and finally eluted with 500 µl of 1% SDS, 0.1 M NaHCO$_3$ (Sigma-Aldrich) solution. DNA was purified by phenol/chloroform procedure. In brief, 500 µl of phenol/chloroform (Panreac AppliChem) was added to the solution containing DNA and stirred vigorously. After centrifugation at $9,300 \times g$ for 10 min, the upper aqueous phase was transferred to a new tube and washed twice with ethanol. Finally, DNA was eluted in 20 µl of water. ChIP analysis was performed by real time-PCR using SYBR Green (Bio-Rad). Promoter occupancy was determined by the percent input method normalized to the condition favoring pluripotency. Primers used are listed in Supplementary Table 1 (available at http://www.cabimer.es/web/docs/grupos/tcmr2/Material SuplementarioCellTrasplantation.zip).

Immunoprecipitation

Cells were trypsinized from culture dishes, centrifuged, and washed once with cold PBS. Cell pellets were then resuspended and incubated in nondenaturing lysis buffer containing 50 mM Tris-HCl (pH 7.4), 300 mM NaCl, 5 mM EDTA, 0.1 mM neocuproine (Sigma-Aldrich), and 1% Triton X-100, supplemented with protease inhibitor cocktail (Sigma-Aldrich) for 45 min on ice and subsequently sonicated with four pulses for 10 s each at 10% amplitude. Following centrifugation, supernatant proteins were quantified by Bradford assay. Samples containing 3 mg of protein were incubated with 3 µg of anti-Jarid-2 (Abcam) for 2 h with stirring at 4°C. Then 70 µl of Dynabeads protein A (Thermo Fisher Scientific) was attached to the complex antibody–proteins overnight at 4°C. The samples were washed three times with nondenaturing lysis buffer for 5 min with stirring at 4°C and washed one last time with 200 µl of 50 mM Tris (pH 8). Proteins were denatured with 50 µl of 1× Laemmli buffer supplemented with 2.5% β-mercaptoethanol, separated by gradient SDS-PAGE (Mini-Protean TGX Gels; 4–15% acrylamide; Bio-Rad), and transferred to PVDF membranes. Finally, membranes were blocked with TBST and 5% nonfat dried milk for 30 min at RT and probed with anti-Jarid-2 (1:1,000; Abcam), anti-P300 (1:1,000; Santa Cruz Biotechnology), and anti-Ezh2 (1:500; BD Biosciences). Secondary antibodies were anti-rabbit IgG (1:20,000; Sigma-Aldrich) and anti-mouse IgG (1:40,000; Jackson ImmunoResearch). Total protein (100 µg) was loaded as a control.

Glucose-Stimulated Insulin Secretion

Clusters were washed two times for 30 min at 37°C with homemade Krebs buffer (135 mM NaCl, 3.6 mM KCl, 5 mM $NaHCO_3$, 10.5 mM $MgCl_2$, 0.5 mM NaH_2PO_4, 2.5 mM $CaCl_2$, 10 mM HEPES, and 0.1% BSA; all Sigma-Aldrich) and were exposed to Krebs buffer containing 3 mM glucose for 1 h, and supernatant was collected. Clusters were then incubated in Krebs buffer containing either 20 mM glucose or 25 mM KCl for 1 h, and supernatant was collected. Insulin release was measured with the Ultrasensitive Mouse Insulin Enzyme-linked Immunosorbent Assay (ELISA) kit (Mercodia, Uppsala, Sweden). DNA of cell clusters was extracted and quantified (Nanodrop ND1000 spectrophotometer; Thermo Fisher Scientific).

Statistical Analyses

Data are means ± standard error of mean (SEM), and comparisons between values were analyzed using one-tailed Student's *t*-test with SigmaPlot software (Systat Software Inc., San Jose, CA, USA). Values of $p < 0.05$ were considered statistically significant.

RESULTS

NO Induces Pdx1 Expression

R1/E mESCs cultured for 3 days in the presence or absence of LIF and 500 μM DETA-NO (19 h) increase Pdx1 expression, both at the mRNA and protein levels (Fig. 1A and B). Dose response experiments show that PDX1 protein levels were significantly increased upon exposure of R1/E and D3 mESCs to 500 μM DETA-NO (supplementary Fig. 1, available at http://www.cabimer.es/web/docs/grupos/tcmr2/MaterialSuplementarioCellTrasplantation.zip). Moreover, immunofluorescence studies reveal that PDX1 is localized in the nuclei (Fig. 1C). The population of cells treated with DETA-NO displays a rightward shift in cytometry plots, thus suggesting an enhanced expression of PDX1 protein (Fig. 1D). Quantification of fluorescence intensity shows that PDX1-positive cells have significantly increased fluorescence following exposure to DETA-NO (Fig. 1E).

Impact of NO on the Epigenetic Changes of Pdx1 *Promoter*

To gain insight into the molecular processes involved in the effect of NO on *Pdx1* expression, analysis of epigenetic changes occurring at the *Pdx1* promoter region was undertaken. Three CpG islands were detected by Methyl Primer Express software (Thermo Fisher Scientific): (−2,000, −1,600), (−350, 650), (1,150, 1,650) bp from the translation start. We focused our study on islands dubbed distal CpG (−2,000, −1,600) and proximal CpG (−350, 650) since it has been reported that the three conserved

and functionally important subdomains (areas I, II, and III) are localized between −2,800 and −1,600[11], and it has been found that methylation of the *Pdx1* proximal promoter (from −275 to +1 bp) is associated with *Pdx1* silencing[12,28] (Fig. 2A). Bisulfite sequencing PCR analysis shows methylation of 47 CpG sites, belonging to both proximal and distal CpG islands. DETA-NO treatment leads to enhanced methylation of CpG sites 8, 22, and 46, and demethylation of CpG site 40 in the presence or absence of LIF (Fig. 2B). The pyrosequencing study shows similar results, with the methylation level of the distal CpG island being higher than the methylation level of the proximal CpG island. The degree of distal CpG island methylation of cells cultured in the presence of LIF is lower than cells cultured in the absence of LIF. Exposure to DETA-NO leads to increased methylation that is similar to the methylation level of INS-1E cells. Regarding the methylation level of the proximal CpG island, cells cultured in the absence of LIF and with DETA-NO present a methylation pattern similar to that of INS-1E cells. This rat cell line was used as a positive control of *Pdx1* expression[29] because they constitute a stable and glucose-responsive β-cell surrogate[30]. Twelve to 16 CpG sites were not analyzed in INS-1E cells because that region is not conserved between mice and rats (Fig. 2C).

On the other hand, histone marks in the proximal region of the *Pdx1* promoter were studied by ChIP. Occupancy of acetylated H3 at the *Pdx1* promoter was studied, and the results show that exposure to DETA-NO does not significantly affect acetylated H3 occupancy (Fig. 2D). By contrast, the occupancy ratio H3K27me3/H3K4me3 was affected by DETA-NO treatment, both in the presence or absence of LIF.

Role of PRC2 in the Regulation of Pdx1 *Expression*

To further investigate the mechanism underlying NO-induced decreases in H3K27me3 occupancy on the *Pdx1* promoter, the expression and function of PRC2 proteins JARID-2 and EZH2 were studied. Results show that while EZH2 does not change its expression following NO treatment, JARID-2 expression is decreased, both at the mRNA and protein levels (Fig. 3A and B). To ascertain if PRC2 directly represses *Pdx1* expression, JARID-2 occupancy at the *Pdx1* proximal promoter was studied by ChIP. The result indicates that JARID-2 is released significantly from the *Pdx1* promoter after DETA-NO treatment (Fig. 3C).

Furthermore, we studied the contribution of histone acetyltransferase P300 to the regulation of *Pdx1* expression. Thus, P300 expression was measured by qRT-PCR and Western blot, and the results indicate that P300 protein is decreased in cells treated with DETA-NO, although there is no change in its mRNA (Fig. 3A and B). In addition, P300 is also released significantly from the *Pdx1* promoter after DETA-NO exposure and in the
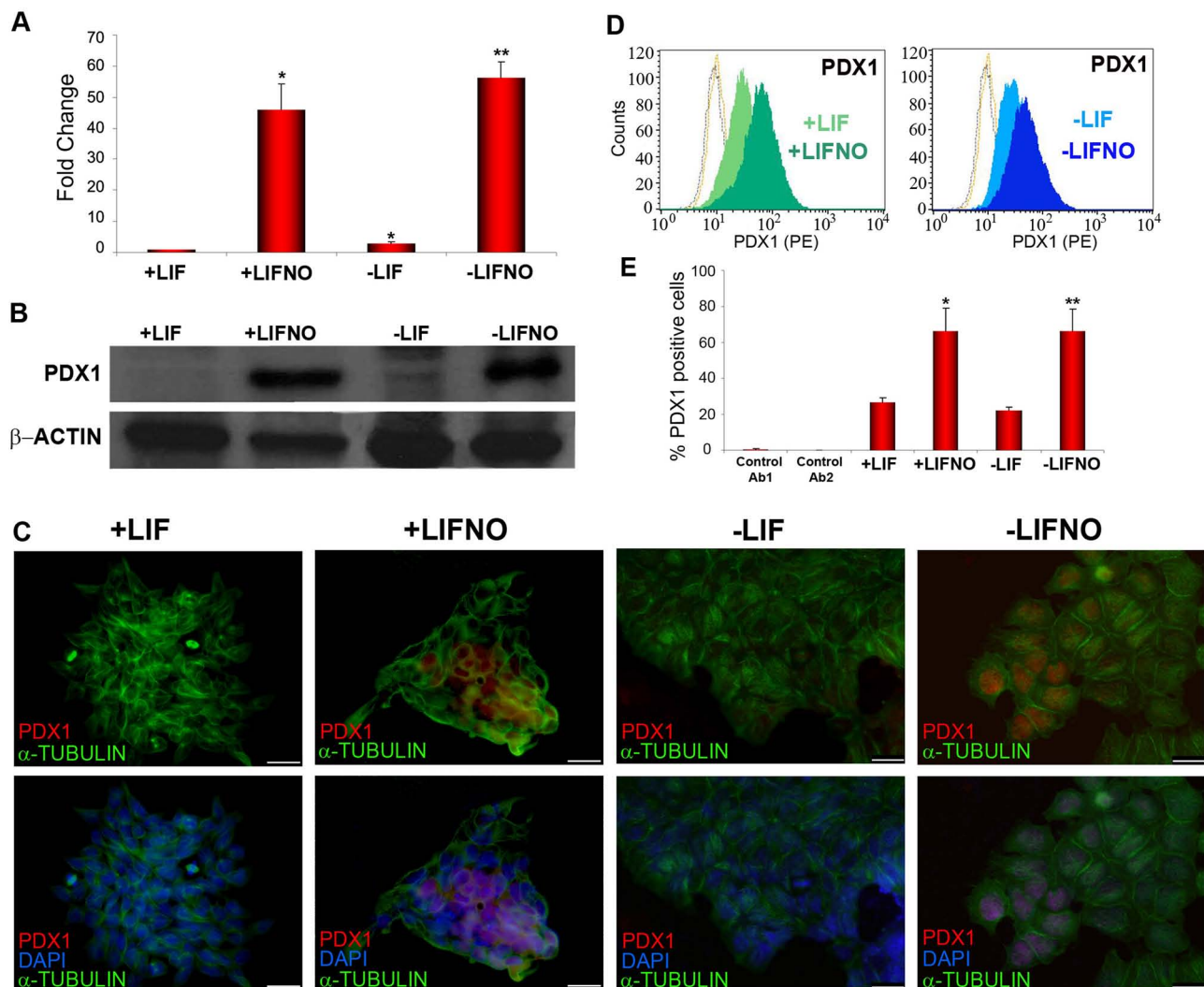
Figure 1. Nitric oxide effects on *Pdx1* expression in R1/E mESCs. (A) Relative expression of *Pdx1* by real-time polymerase chain reaction (PCR). These values are normalized to the expression values of *β-actin*, used as loading control and analyzed using the $\Delta\Delta$Ct algorithm. It represents an average of three independent experiments. Data are presented as mean ± SEM. The *y*-axis corresponds to relative expression level of *Pdx1* (fold change). (B) Western blot of PDX1. It shows the results of Western blot of PDX1 in the four culture conditions. β-Actin was used as loading control. The blot is representative of three independent experiments. (C) PDX1 immunofluorescence. Images show cells cultured in the four conditions and subsequently stained with DAPI (blue), PDX1 (red), and α-tubulin (green). Scale bars: 25 μM. The images shown are representative of three independent experiments. (D) Flow cytometry of PDX1. The green graph shows the +LIF conditions, and the blue graph shows the −LIF conditions. (E) Flow cytometry of PDX1. The graph represents the percentage of Pdx1-positive cells in the four culture conditions and negative controls, primary, and secondary antibodies. (A and E) *$p < 0.05$ statistically significant versus cells cultured in the presence of LIF, **$p < 0.05$ versus cells cultured in the presence and absence of LIF. +LIF: cells cultured in the presence of LIF; +LIFNO: cells cultured in the presence of LIF plus 500 μM DETA-NO; −LIF: cells cultured without LIF; −LIFNO: cells cultured without LIF plus 500 μM DETA-NO. In the four conditions, cells are cultured for 4 days and with DETA-NO for 19 h.

absence of LIF (Fig. 3C). In order to test the relevance of P300 in repressing *Pdx1*, DETA-NO-exposed cells were treated with the P300 inhibitor (P300i) and a synergistic effect of both molecules on *Pdx1* expression was observed (Fig. 3E). Furthermore, ChIP studies corroborate that JARID-2 and P300 occupy the same region on the *Pdx1* promoter. Finally, coimmunoprecipitation reveals that P300 interacts with PRC2 at the *Pdx1* promoter region (Fig. 3D).

Optimized Protocol to Generate Insulin-Producing Cells

In view of the relevance of P300 on the regulation of *Pdx1* expression, a modification of a protocol developed previously
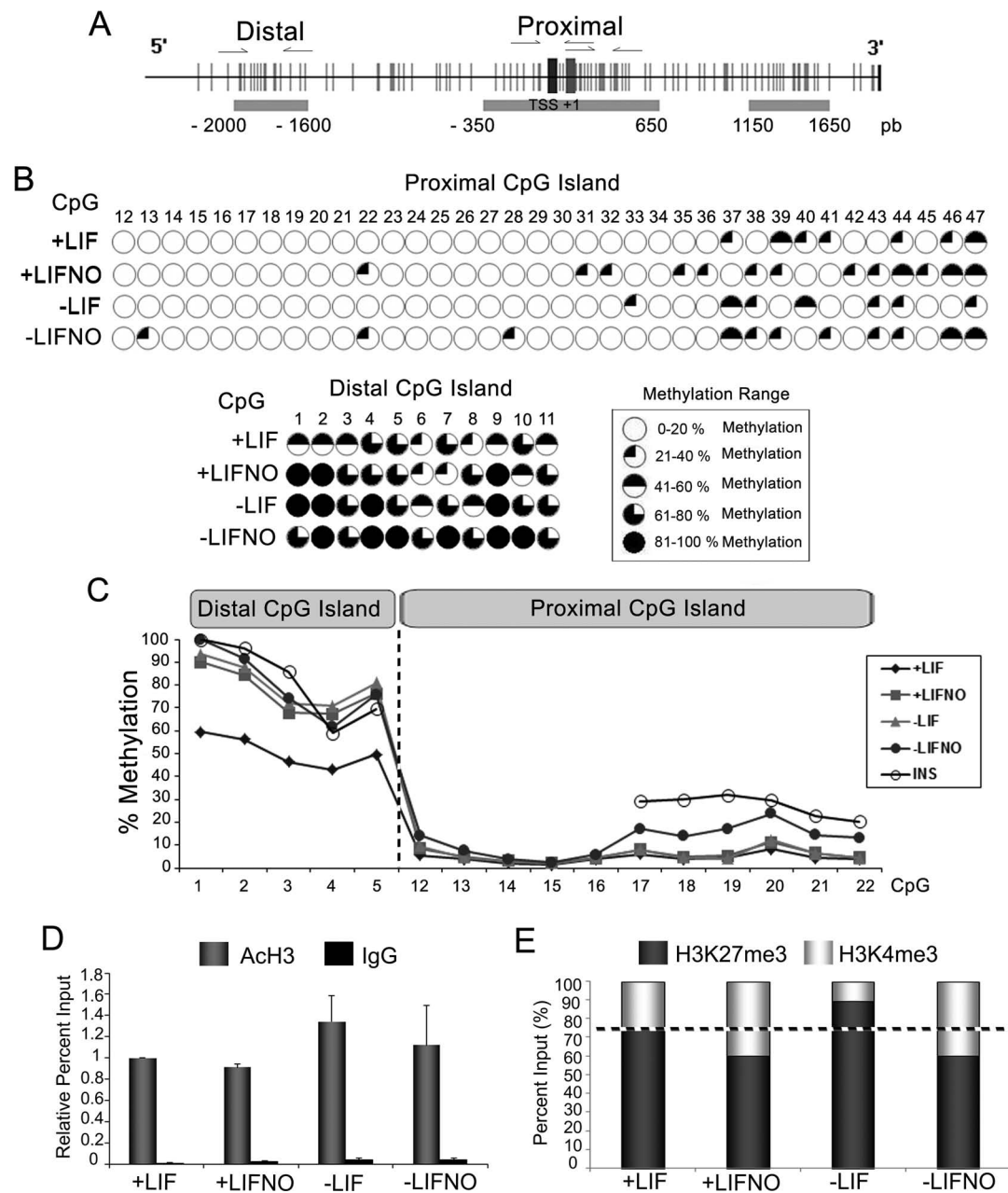
Figure 2. Analysis of epigenetic changes of *Pdx1* promoter. (A) *Pdx1* promoter scheme. This image shows the *Pdx1* promoter and gene. Horizontal gray rectangles represent CpG islands, and vertical lines are the CpG sites. Vertical gray rectangles represent the transcription start (TSS) and the translation start (+1). The arrows represent the pairs of primers designed to amplify the regions of interest. (B) Methylation analysis of distal CpG island and proximal CpG island by BSP. It shows the CpG sites studied (distal CpG island and proximal CpG island). These sites are represented by circles: white circles, those CpG sites whose percentage of methylation is very low or even zero; black circles, those CpG sites whose methylation level is high or complete. Among them, there is a gradient of methylation that is shown in the inset of the image. (C) Methylation analysis of distal CpG islands and proximal CpG islands by bisulfite pyrosequencing. This graph represents the percentage of methylation of studied CpG sites. Diamonds: R1/E cells cultured in the presence of LIF. Squares: R1/E cells cultured in the presence of LIF plus 500 μM DETA-NO. Triangles: R1/E cells cultured in the absence of LIF. Full circles: R1/E cells cultured without LIF plus 500 μM DETA-NO. Open circles: INS-1E cells whose methylation level was used as control. (D) Analysis of acetylated H3 occupancy at *Pdx1* by chromatin immunoprecipitation assay (ChIP). This graph represents ChIP analysis for acetylated H3 expressed as relative percent input (relativized to the condition favoring cell pluripotency) of three independent experiments. Data are mean ± SEM. (E) Stacked bars for bivalent mark dynamics of H3K27me3 and H3K4me3. They represent an average of three independent experiments. +LIF: cells cultured in the presence of LIF; +LIFNO: cells cultured in the presence of LIF plus 500 μM DETA-NO; −LIF: cells cultured in the absence of LIF; −LIFNO: cells cultured without LIF plus 500 μM DETA-NO. In the four conditions tested, cells are cultured for 4 days and with DETA-NO for 19 h.
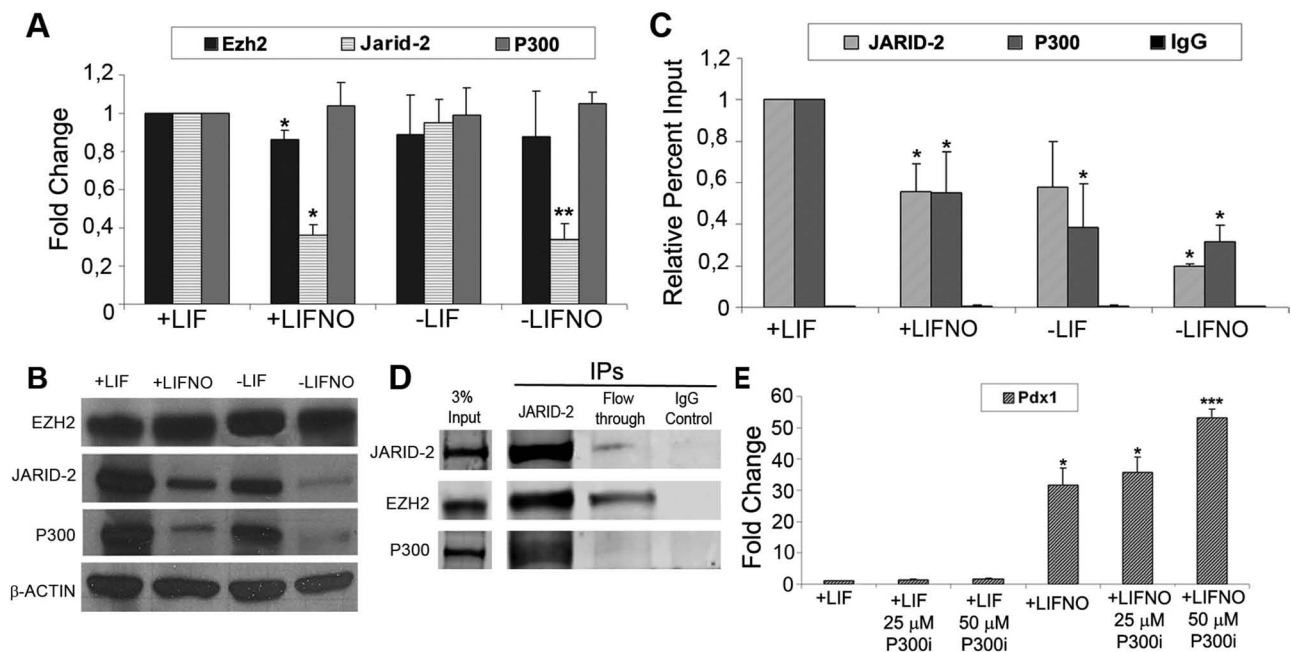
Figure 3. Studies on polycomb repressive complex (PRC2) in R1/E mESCs. (A) Study of PRC2 and P300 expression by real-time PCR. Values are normalized to the expression of β-actin and analyzed using the $\Delta\Delta$Ct algorithm. It represents an average of three independent experiments. Data are mean $\pm$ SEM. The y-axis corresponds to relative expression level (fold change). (B) Study of PRC2 and P300 expression by Western Blotting. The image shown is representative of three independent experiments. β-Actin was used as a loading control. (C) Analysis of JARID-2 and P300 occupancy at *Pdx1* proximal promoter by ChIP. Data are mean $\pm$ SEM of three independent experiments. The y-axis corresponds to relative percent input from undifferentiated cells. (D) Coimmunoprecipitation assay of JARID-2, EZH2, and P300. Three percent of total coimmunoprecipitated protein was loaded as input. Proteins not retained to complex agarose beads and Jarid-2 antibody were loaded as control of immunoprecipitation grade (Flow through). An immunoprecipitation with IgG antibody was developed as control of nonspecific binding (IgG control). (E) *Pdx1* expression analysis by real-time PCR. Data are normalized to the expression values of β-actin, used as loading control and analyzed using the $\Delta\Delta$Ct algorithm. Data are mean $\pm$ SEM of three independent experiments. The y-axis corresponds to relative expression level of *Pdx1* (fold change). *$p < 0.05$ versus cells cultured in the presence of LIF, **$p < 0.05$ versus cells cultured in the presence and absence of LIF, ***$p < 0.05$ versus cells cultured in the presence of LIF plus 500 μM DETA-NO. +LIF: cells cultured in the presence of LIF; +LIFNO: cells cultured in the presence of LIF plus 500 μM DETA-NO; −LIF: cells cultured without LIF; −LIFNO: cells cultured without LIF plus 500 μM DETA-NO. In the four conditions cells were cultured for 4 days and with DETA-NO for 19 h.

was implemented[6]. The modification consisted of the addition of P300i (C646) after treatment with valproic acid and before growth in suspension for 3 days (Fig. 4A). Cell morphology and fate were affected after every step of the protocol. Thus, exposure to DETA-NO led to substantial cell death, and the surviving cells acquired an epithelial morphology. Following exposure to valproic acid, groups of cells formed colonies with a round and shiny morphology, while others remained scattered and dull. Addition of P300i provoked considerable cell death, but surviving cells formed cluster-like structures. Finally, culture in suspension led to the formation of islet-like clusters (Fig. 4B). Analysis of expression markers revealed that DETA-NO treatment led to an increase in *Pdx1, Nkx6.1, Nkx2.2, Ptf1a,* and *Glut2* mRNA (Fig. 4C and D). Interestingly, NO also increased pre-mRNA *Ins1* levels (Fig. 4C). Valproic acid treatment enhanced the expression of definitive endoderm genes, including SRY (sex-determining region Y)-box 17 (*Sox17*), forkhead box A2

(*FoxA2*), HNF1 homeobox B (*Hnf1b*), and NK2 homeobox 2 (*Nkx2.2*). At day 10, there was a decrease in *Pdx1* expression, which was recovered by exposure to P300i. Moreover, P300i also enhanced *Pax4* expression. At the end of the differentiation protocol, markers of definitive endoderm (*Sox17*, *Foxa2*, and *Hnf1b*) and some markers of pancreatic progenitors (*Pdx1*, *Pax4*, *Nkx6.1*, *Nkx2.2*, *Kir6.2*, *GcK*, *Ins1*, and *Glut2*) were also upregulated (Fig. 4D). Cluster formation has been reported to improve long-term maintenance of human islets in vitro[31] and to increase the percentage of insulin-expressing cells in differentiation protocols[32]. Moreover, suspension culture enables uniformity of cellular composition, and pancreatic aggregates can be implanted without disrupting the maturing cellular architecture[33]. In our protocol, it is interesting to note that these cells were negative for *Gcg*, *Amy2*, and *Sst* (Fig. 4C). Immunofluorescence revealed that most cells expressed PDX1 and GLUT2, and some of them were positive for C-peptide (Fig. 5A).
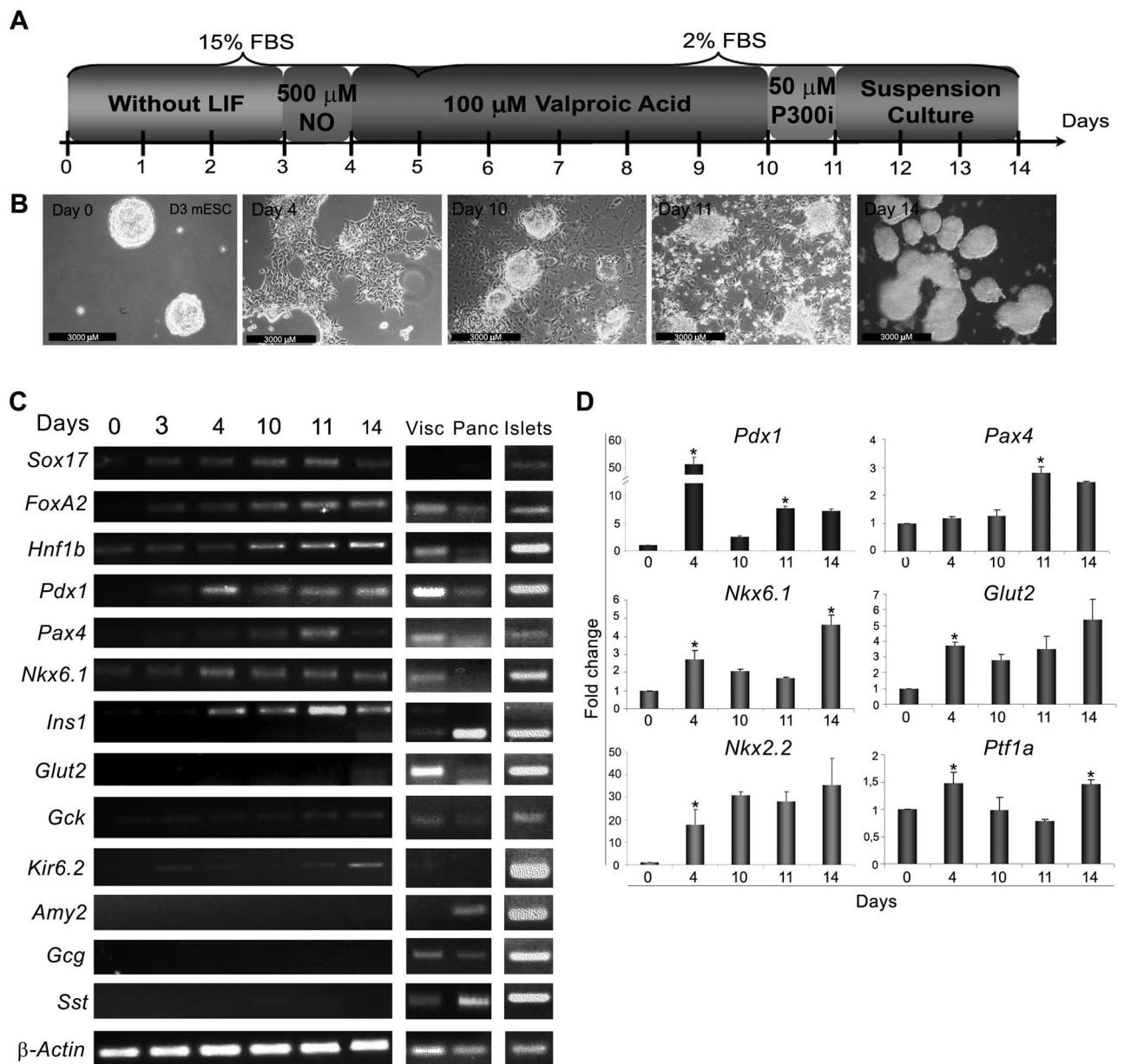
Figure 4. Differentiation protocol to generate insulin-producing cells from mESCs. (A) Differentiation protocol scheme showing the culture conditions. (B) Bright-field images showing colony morphology of D3 mESCs during the differentiation protocol. Scale bars: 3,000 μm. (C) Qualitative analysis by RT-PCR for pancreatic markers for each step of differentiation protocol. Visc: embryo viscera, Panc: adult pancreas, Islets: mouse islets were used as a control. *β-Actin* was used as loading control cDNA. The image shown is representative of three to five independent experiments. (D) Quantitative analysis by real-time PCR for pancreatic markers. These values are normalized to the expression values of β-actin, used as loading control and analyzed using the ΔΔCt algorithm. Data shown are mean ± SEM of three independent experiments. The *y*-axis corresponds to relative expression (fold change). *$p < 0.05$ statistically significant from the previous day of the differentiation protocol shown.

A key functional feature of β cells is the ability to release insulin in response to secretagogues. Cell clusters generated with the protocol reported here display responsiveness to both high glucose and KCl (Fig. 5B). A summary of the findings reported here on Pdx1 regulation and its contribution to the differentiation of mESCs into insulin-producing cells is shown in Figure 6.

DISCUSSION

Pdx1 is a transcription factor necessary for pancreatic development and β-cell maturation and exhibits a
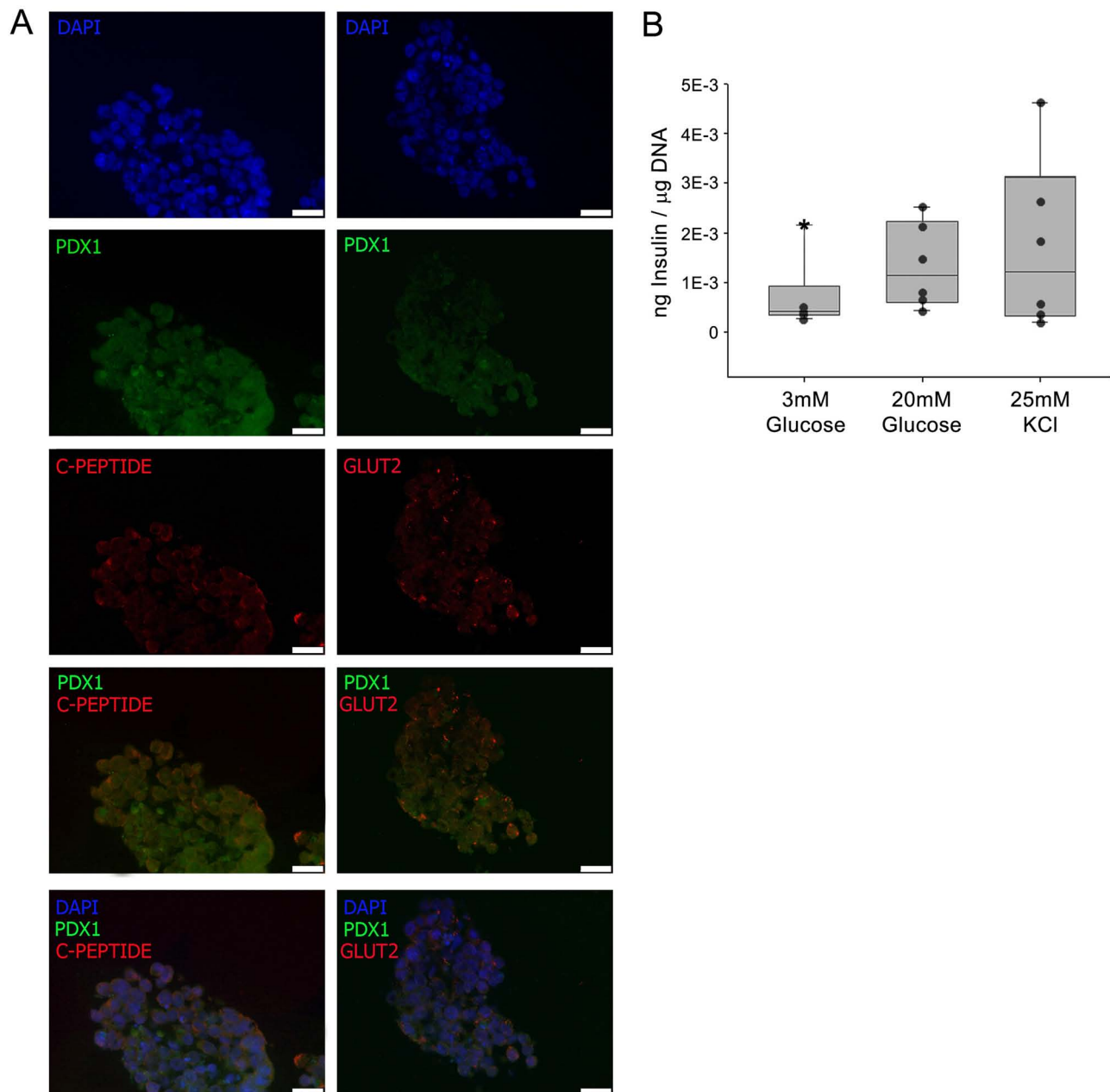
Figure 5. Islet-like clusters generated by differentiation protocol. (A) Immunofluorescence of islet-like clusters obtained by directed differentiation of D3 mESCs. Left: Immunofluorescence of DAPI (blue), PDX1 (green), and C-peptide (red). Right: Immunofluorescence of DAPI (blue), PDX1 (green), and GLUT2 (red). Scale bars: 25 μM. (B) Box and whiskers plot of secreted insulin from differentiated islet-like clusters from mESCs. Each black circle is the value for an experiment ($n=6$). Insulin secretion (ng insulin/μg DNA) at 3 mM glucose ranged from 2.74E−4 to 2.15E−3 (*) and 4.31E−4 to 2.53E−3 at 20 mM glucose. At 25 mM KCl, the values ranged from 2.01E−4 to 4.61E−3. * denotes an outlier. The thick horizontal line denotes the median.

biphasic pattern of expression during pancreatic development[34]. An appropriate regulation of its expression might be instrumental for the generation of insulin-producing cells from pluripotent stem cells. The present study shows that exposure of mESCs to 500 μM DETA-NO leads to enhanced and transient expression of Pdx1. It has been previously reported that NO induces epigenetic changes such as DNA methylation[35]. In fact, methylation of the proximal CpG island of the *Pdx1* promoter is associated with *Pdx1* silencing in intrauterine growth retardation (IUGR)[12,28]. Therefore, we studied the methylation degree of the *Pdx1* promoter by BSP
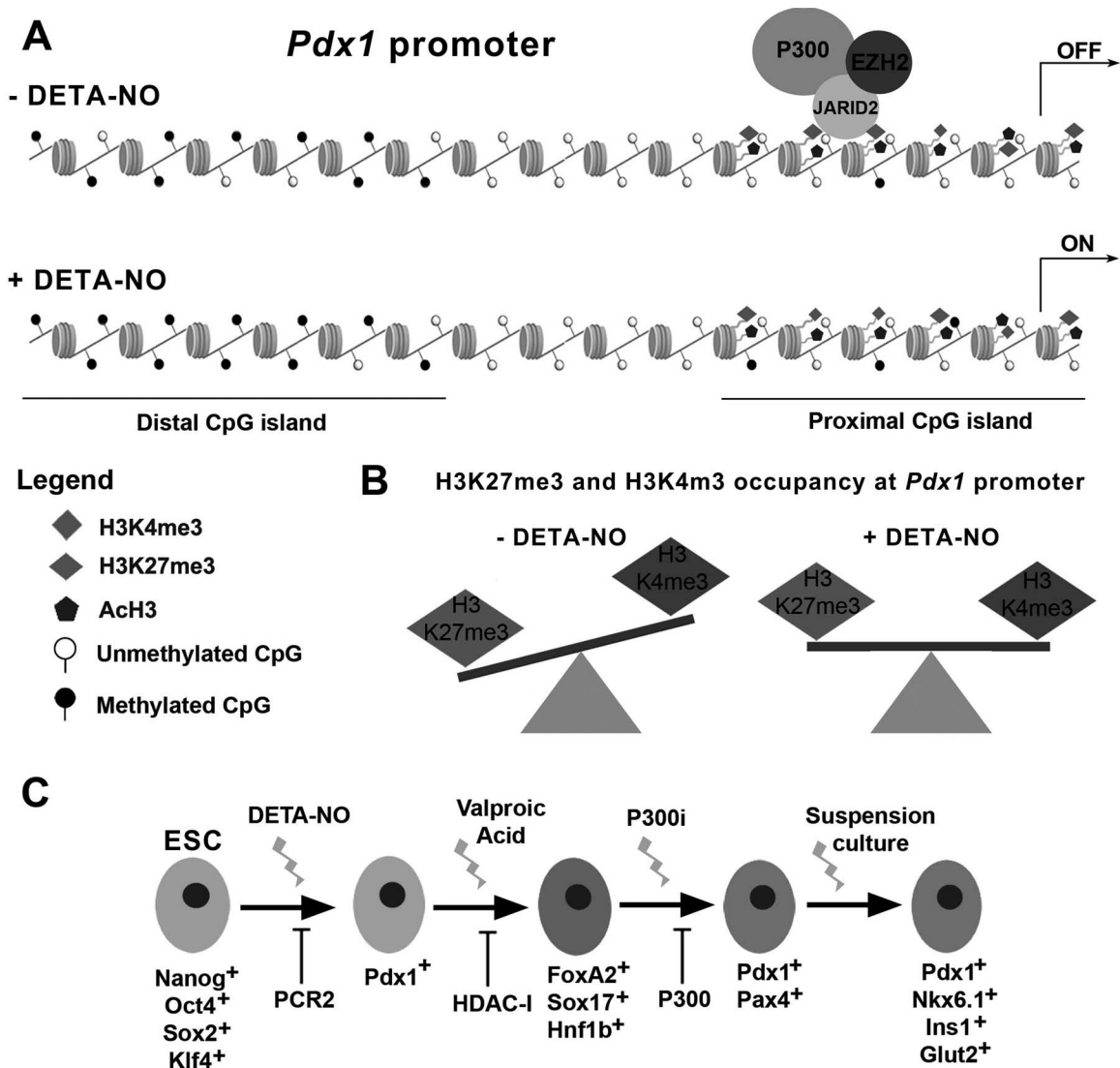
Figure 6. Overview of *Pdx1* regulation by NO and its contribution to the generation of insulin-producing cells from mESCs. (A) *Pdx1* promoter in untreated mESCs and after NO treatment. In untreated mESCs, *Pdx1* gene expression is repressed by PRC2, which leads to a high occupancy of H3K27me3. NO treatment causes the release of PRC2 and P300 from the *Pdx1* promoter, thus allowing gene expression. Acetylation of H3 remains constant while minor changes in DNA methylation are produced. (B) NO treatment modifies the histone marks over the *Pdx1* promoter. Exposure to DETA-NO (500 μM) decreases the ratio H3K27me3/H3K4me3. (C) Protocol for mESC differentiation into insulin-producing cells. NO treatment releases PRC2 from the *Pdx1* promoter and *Pdx1* is expressed. Expression of endoderm lineage genes (*FoxA2*, *Sox17*, and *Hnf1β*) is observed after valproic acid treatment. Thus, addition of valproic acid (HDAC-I inhibitor) allows that chromatin to remain open and helps to differentiate cells into pancreatic lineage cells. In a later stage, inhibition of P300 stimulates the expression of pancreatic progenitor markers such as *Pdx1* and *Pax4*. Finally, culture in suspension allows the formation of islets-like clusters, thus enabling a stable expression of β-cell markers *Pdx1*, *Nkx6.1*, *Glut2*, and *Ins1*.

and pyrosequencing. The studies show that the proximal CpG island represents less than 20% of overall methylation, while methylation of the distal island represents more than 60%. Methylation levels of both islands are slightly increased after NO treatment, despite the significantly increased expression of the gene. Thus, it is entirely possible that methylation of the *Pdx1* promoter might represent a poised state of *Pdx1* during

differentiation of mESCs. On the other hand, methylation induced by NO treatment in mESCs is similar to the pattern observed in the glucose-responsive β-cell line (INS-1E). The fact that only conserved sequences in the promoter region undergo changes in the degree of methylation supports a possible role for this modification in the epigenetic regulation of *Pdx1* gene expression. Furthermore, the level of methylation of the

proximal promoter in undifferentiated mESCs reported here is in accordance with those reported in rodent models of IUGR, a condition associated with the onset of type 2 diabetes[12,28]. Factors other than methylation might control *Pdx1* expression in ESCs. It has been reported that genes encoding key lineage-specific regulators are marked by both H3K4me3 and H3K27me3, creating a bivalent state in which genes are poised for future activation but remain inactive until the repressive mark is removed[36]. ChIP data reported here on H3K27me3 and H3K4me3 occupancy agree with studies on bivalency during pancreatic differentiation, in which H3K4me3 and H3K27me3 modifications were mapped in human embryonic stem cells (hESCs) at defined stages during pancreatic endocrine differentiation[3,37]. The balance in the occupancy of both marks at the *Pdx1* promoter changes after treatment with NO. Thus, in the presence of LIF, NO increases H3K4me3 occupancy from 25% to 40%, and in the absence of LIF increases from 10% to 40%. These results are in agreement with other studies showing progressive decline in the H3K27me3/H3K4me3 occupancy ratio at the *Pdx1* promoter during pancreatic development[23]. In the same light, acetylated H3 occupancy at the proximal *Pdx1* promoter is not altered by NO treatment. The persistence of both AcH3 and H3K27me3 marks on the silent *Pdx1* has been previously described in hepatoblasts[24,38,39]. It is possible that the presence of acetylated H3 at the *Pdx1* promoter could also contribute to the poised state of this gene during early stages of pancreatic development.

It has been reported that removal of the polycomb group (PcG)-mediated repression on stage-specific genes is the key regulator during development[23]. PcG proteins have an important role in controlling the expression of genes essential for development, differentiation, and maintenance of cell fates[14,31,40]. In the present work, we studied the role of components of PRC2 on *Pdx1* expression in mESCs. NO treatment decreases JARID-2 expression, which is essential for binding of the PRC2 to target genes in ESCs[18]. We report here that JARID-2 is found on the *Pdx1* promoter in the presence of LIF and is released from the promoter after LIF withdrawal and NO treatment. mESCs contain high levels of JARID-2 protein that interact with and stabilize PRC2 at target genes[17,18]. We detected JARID-2/EZH2 complexes under conditions favoring cell pluripotency, thus suggesting that binding of the PRC2 complex on the *Pdx1* promoter is involved in its repression. This finding is consistent with studies showing that JARID-2 and EZH2 are bound at the *Pdx1* promoter in ESCs and that JARID-2 silencing allows higher *Pdx1* expression and lower EZH2 occupancy[17,24]. It has also been reported that PRC2 regulates transcriptional repression by catalyzing the di- and trimethylation of lysine 27 on histone H3 (H3K27me2/3)[20,41]. In this

regard, the studies shown here indicate that NO-driven release of JARID-2 is linked to changes in the H3K27me3/H3K4me3 balance at the *Pdx1* promoter.

Moreover, it has been shown that P300 is necessary for acetylation of liver-specific regulatory elements and full liver-specific gene activation and that P300 modulates the specification of liver progenitors instead of pancreas progenitors[24]. Here we show that P300 occupancy represses *Pdx1* expression in undifferentiated mESCs, and that during cell differentiation P300 is released from the *Pdx1* promoter. Likewise, chemical inhibition of P300 leads to higher expression of PDX1 in cells cultured with LIF and DETA-NO when compared with cells cultured with LIF and DETA-NO. Moreover, pull-down experiments with JARID-2 and EZH2 show that P300 interacts with PRC2 complex in undifferentiated conditions. These results are in agreement with those from previous studies that showed that P300 can act as a repressor independently of its acetyltransferase activity[25,26,42,43]. Possible posttranslational modifications such as a SUMO-dependent repression[25] or recruitment of other repressive components such as HDAC6 or HDAC1[26] remain to be studied.

On the basis of the knowledge that P300 is a repressor of the *Pdx1* gene and the mechanisms controlling the expression of *Pdx1* in mESCs, a differentiation protocol was designed to generate insulin-producing cells. Previously, we reported the generation of definitive endoderm cells with a protocol consisting of sequential exposure to DETA-NO, serum withdrawal, and treatment with valproic acid[6]. The novel small molecule-based protocol presented here consists of five steps in which cells are differentiated toward functional insulin-producing cells in a full in vitro system. The expression of Pdx1 by removal of P300 repression is instrumental for the development of β-cell surrogates, and the combined use of small molecules such NO and valproic acid leads to sequential activation of signals relevant for induction of pancreatic lineage cells. The generation of cell aggregates with pancreatic progenitor cells at 11 days expressing *Pdx1* and *Pax4* prepared the cells for a consistent maturation step. At the end of the protocol (14 days), cells expressing β-cell markers such as *Pdx1*, *Nkx6.1*, *GcK*, *Kir6.2*, *Glut2*, and *Ins1* were capable of responding to secretagogues such as high glucose and KCl.

β-Catenin, activin/nodal, and bone morphogenetic protein (BMP) signaling pathways are known to have an important role during endoderm generation. Thus, activin A is used to activate nodal signaling, and Wnt activators or a BMP antagonist such as noggin is commonly used for definitive endoderm induction from human pluripotent stem cells[44–46]. Another key step is generation of functional hormone-secreting cells. A considerable number of molecules have been proven to be "maturation factors" such insulin-like growth factor 1 (IGF-1), exendin-4, hepatocyte growth factor (HGF), B27 supplement, betacellulin, or nicotinamide[3,47,48].

Relevant progress in the field has been reported by Rezania et al.[48]. They have generated in vitro functional β-like cells, which permanently reverse hyperglycemia when transplanted into diabetic mice. Alternatively, Pagliuca et al. have reported a strategy for large-scale production of functional human β cells from human pluripotent stem cells generating glucose-responsive and monohormonal insulin-producing cells[8]. The increasing number of protocols to generate β-cell surrogates from ESCs underscores the collective effort made over the past 10 years to generate efficient and reproducible methods to obtain fully responsive β cells in vitro. The findings reported here indicate that promoting the expression of Pdx1 by removal of PRC2 and P300 repression is instrumental for the development of β-cell surrogates. The combined use of small molecules such as DETA-NO, valproic acid, and P300 inhibitor leads to sequential activation of signals important for pancreatic lineage specification. Subsequent formation of cell aggregates enables the generation of glucose-responsive monohormonal insulin-producing cells. This protocol is a promising tool for efficient generation of β cells from pluripotent stem cells, but further testing is needed to determine whether these findings are also applicable for human stem cells.

REFERENCES

1. Soria B, Roche E, Berna G, Leon-Quinto T, Reig JA, Martin F. Insulin-secreting cells derived from embryonic stem cells normalize glycemia in streptozotocin-induced diabetic mice. Diabetes 2000;49(2):157–62.

2. Leon-Quinto T, Jones J, Skoudy A, Burcin M, Soria B. In vitro directed differentiation of mouse embryonic stem cells into insulin-producing cells. Diabetologia 2004;47(8):1442–51.

3. D'Amour KA, Bang AG, Eliazer S, Kelly OG, Agulnick AD, Smart NG, Moorman MA, Kroon E, Carpenter MK, Baetge EE. Production of pancreatic hormone-expressing endocrine cells from human embryonic stem cells. Nat Biotechnol. 2006;24(11):1392–401.

4. Kroon E, Martinson LA, Kadoya K, Bang AG, Kelly OG, Eliazer S, Young H, Richardson M, Smart NG, Cunningham J, Agulnick AD, D'Amour KA, Carpenter MK, Baetge EE. Pancreatic endoderm derived from human embryonic stem

5. Zhang D, Jiang W, Liu M, Sui X, Yin X, Chen S, Shi Y, Deng H. Highly efficient differentiation of human ES cells and iPS cells into mature pancreatic insulin-producing cells. Cell Res. 2009;19(4):429–38.

6. Mora-Castilla S, Tejedo JR, Hmadcha A, Cahuana GM, Martin F, Soria B, Bedoya FJ. Nitric oxide repression of Nanog promotes mouse embryonic stem cell differentiation. Cell Death Differ. 2010;17(6):1025–33.

7. Bruin JE, Erener S, Vela J, Hu X, Johnson JD, Kurata HT, Lynn FC, Piret JM, Asadi A, Rezania A, Kieffer TJ. Characterization of polyhormonal insulin-producing cells derived in vitro from human embryonic stem cells. Stem Cell Res. 2014;12(1):194–208.

8. Pagliuca FW, Millman JR, Gurtler M, Segel M, Van Dervort A, Ryu JH, Peterson QP, Greiner D, Melton DA. Generation of functional human pancreatic beta cells in vitro. Cell 2014;159(2):428–39.

9. Stoffers DA, Zinkin NT, Stanojevic V, Clarke WL, Habener JF. Pancreatic agenesis attributable to a single nucleotide deletion in the human IPF1 gene coding sequence. Nat Genet. 1997;15(1):106–10.

10. Ahlgren U, Jonsson J, Edlund H. The morphogenesis of the pancreatic mesenchyme is uncoupled from that of the pancreatic epithelium in IPF1/PDX1-deficient mice. Development 1996;122(5):1409–16.

11. Gerrish K, Van Velkinburgh JC, Stein R. Conserved transcriptional regulatory domains of the pdx-1 gene. Mol Endocrinol. 2004;18(3):533–48.

12. Park JH, Stoffers DA, Nicholls RD, Simmons RA. Development of type 2 diabetes following intrauterine growth retardation in rats is associated with progressive epigenetic silencing of Pdx1. J Clin Invest. 2008;118(6):2316–24.

13. Simon JA, Kingston RE. Mechanisms of polycomb gene silencing: Knowns and unknowns. Nat Rev Mol Cell Biol. 2009;10(10):697–708.

14. Schuettengruber B, Chourrout D, Vervoort M, Leblanc B, Cavalli G. Genome regulation by polycomb and trithorax proteins. Cell 2007;128(4):735–45.

15. Lee TI, Jenner RG, Boyer LA, Guenther MG, Levine SS, Kumar RM, Chevalier B, Johnstone SE, Cole MF, Isono K, Koseki H, Fuchikami T, Abe K, Murray HL, Zucker JP, Yuan B, Bell GW, Herbolsheimer E, Hannett NM, Sun K, Odom DT, Otte AP. Control of developmental regulators by Polycomb in human embryonic stem cells. Cell 2006;125(2):301–13.

16. Boyer LA, Plath K, Zeitlinger J, Brambrink T, Medeiros LA, Lee TI, Levine SS, Wernig M, Tajonar A, Ray MK, Bell GW, Otte AP, Vidal M, Gifford DK, Young RA, Jaenisch R. Polycomb complexes repress developmental regulators in murine embryonic stem cells. Nature 2006;441(7091):349–53.

17. Peng JC, Valouev A, Swigut T, Zhang J, Zhao Y, Sidow A, Wysocka J. Jarid2/Jumonji coordinates control of PRC2 enzymatic activity and target gene occupancy in pluripotent cells. Cell 2009;139(7):1290–302.

18. Pasini D, Cloos PA, Walfridsson J, Olsson L, Bukowski JP, Johansen JV, Bak M, Tommerup N, Rappsilber J, Helin K. JARID2 regulates binding of the Polycomb repressive complex 2 to target genes in ES cells. Nature 2010;464(7286):306–10.

19. Loh YH, Wu Q, Chew JL, Vega VB, Zhang W, Chen X, Bourque G, George J, Leong B, Liu J, Wong KY, Sung, KW, Lee CWH, Zhao XD, Chiu KP, Lipovich L, Kuznetsov VA, Robson P, Stanton LW, Wei CL, Ruan Y, Lim B, Ng HH. The Oct4 and Nanog transcription network regulates

pluripotency in mouse embryonic stem cells. Nat Genet. 2006;38(4):431–40.

20. Landeira D, Sauer S, Poot R, Dvorkina M, Mazzarella L, Jorgensen HF, Pereira CF, Leleu M, Piccolo FM, Spivakov M, Brookes E, Pombo A, Fisher C, Skarnes WC, Snoek T, Bezstarosti K, Demmers J, Klose RJ, Casanova M, Tavares L, Brockdorff N, Merkenschlager M, Fisher AG. Jarid2 is a PRC2 component in embryonic stem cells required for multi-lineage differentiation and recruitment of PRC1 and RNA Polymerase II to developmental regulators. Nat Cell Biol. 2010;12(6):618–24.

21. Kim J, Chu J, Shen X, Wang J, Orkin SH. An extended transcriptional network for pluripotency of embryonic stem cells. Cell 2008;132(6):1049–61.

22. Boyer LA, Lee TI, Cole MF, Johnstone SE, Levine SS, Zucker JP, Guenther MG, Kumar RM, Murray HL, Jenner RG, Gifford DK, Melton DA, Jaenisch R, Young RA. Core transcriptional regulatory circuitry in human embryonic stem cells. Cell 2005;122(6):947–56.

23. Xie R, Everett LJ, Lim HW, Patel NA, Schug J, Kroon E, Kelly OG, Wang A, D'Amour KA, Robins AJ, Won KJ, Kaestner KH, Sander M. Dynamic chromatin remodeling mediated by polycomb proteins orchestrates pancreatic differentiation of human embryonic stem cells. Cell Stem Cell 2013;12(2):224–37.

24. Xu CR, Cole PA, Meyers DJ, Kormish J, Dent S, Zaret KS. Chromatin «prepattern» and histone modifiers in a fate choice for liver and pancreas. Science 2011;332(6032):963–6.

25. Girdwood D, Bumpass D, Vaughan OA, Thain A, Anderson LA, Snowden AW, Garcia-Wilson E, Perkins ND, Hay RT. P300 transcriptional repression is mediated by SUMO modification. Mol Cell 2003;11(4):1043–54.

26. Ma H, Nguyen C, Lee KS, Kahn M. Differential roles for the coactivators CBP and p300 on TCF/beta-catenin-mediated survivin gene expression. Oncogene 2005;24(22):3619–31.

27. Tejedo JR, Tapia-Limonchi R, Mora-Castilla S, Cahuana GM, Hmadcha A, Martin F, Bedoya FJ, Soria B. Low concentrations of nitric oxide delay the differentiation of embryonic stem cells and promote their survival. Cell Death Dis. 2010;1:e80.

28. Pinney SE, Jaeckle Santos LJ, Han Y, Stoffers DA, Simmons RA. Exendin-4 increases histone acetylase activity and reverses epigenetic modifications that silence Pdx1 in the intrauterine growth retarded rat. Diabetologia 2011; 54(10):2606–14.

29. Liu J, Liu Y, Wang H, Hao H, Han Q, Shen J, Shi J, Li C, Mu Y, Han W. Direct differentiation of hepatic stem-like WB cells into insulin-producing cells using small molecules. Sci Rep. 2013;3:1185.

30. Merglen A, Theander S, Rubi B, Chaffard G, Wollheim CB, Maechler P. Glucose sensitivity and metabolism-secretion coupling studied during two-year continuous culture in INS-1E insulinoma cells. Endocrinology 2004;145(2):667–78.

31. Zhao M, Christie MR, Heaton N, George S, Amiel S, Cai Huang G. Amelioration of streptozotocin-induced diabetes in mice using human islet cells derived from long-term culture in vitro. Transplantation 2002;73(9):1454–60.

32. Segev H, Fishman B, Ziskind A, Shulman M, Itskovitz-Eldor J. Differentiation of human embryonic stem cells into insulin-producing clusters. Stem Cells 2004;22(3):265–74.

33. Schulz TC, Young HY, Agulnick AD, Babin MJ, Baetge EE, Bang AG, Bhoumik A, Cepa I, Cesario RM, Haakmeester C, Kadoya K, Kelly JR, Kerr J, Martinson LA, McLean AB, Moorman MA, Payne JK, Richardson M, Ross KG, Sherrer ES, Song X, Wilson AZ. A scalable system for production of functional pancreatic progenitors from human embryonic stem cells. PLoS One 2012;7(5):e37004.

34. Bernardo AS, Cho CH, Mason S, Docherty HM, Pedersen RA, Vallier L, Docherty K. Biphasic induction of Pdx1 in mouse and human embryonic stem cells can mimic development of pancreatic beta-cells. Stem Cells 2009;27(2):341–51.

35. Hmadcha A, Bedoya FJ, Sobrino F, Pintado E. Methylation-dependent gene silencing induced by interleukin 1beta via nitric oxide production. J Exp Med. 1999;190(11):1595–604.

36. Bernstein BE, Mikkelsen TS, Xie X, Kamal M, Huebert DJ, Cuff J, Fry B, Meissner A, Wernig M, Plath K, Jaenisch R, Wagschal A, Feil R, Schreiber SL, Lander ES. A bivalent chromatin structure marks key developmental genes in embryonic stem cells. Cell 2006;125(2):315–26.

37. Kadowaki M, Yoshioka H, Kamitani H, Watanabe T, Wade PA, Eling TE. DNA methylation-mediated silencing of nonsteroidal anti-inflammatory drug-activated gene (NAG-1/GDF15) in glioma cell lines. Int J Cancer 2012;130(2):267–77.

38. Azuara V, Perry P, Sauer S, Spivakov M, Jorgensen HF, John RM, Gouti M, Casanova M, Warnes G, Merkenschlager M, Fisher AG. Chromatin signatures of pluripotent cell lines. Nat Cell Biol. 2006;8(5):532–8.

39. Rojas A, Khoo A, Tejedo JR, Bedoya FJ, Soria B, Martin F. Islet cell development. Adv Exp Med Biol. 2010;654:59–75.

40. Schwartz YB, Pirrotta V. Polycomb silencing mechanisms and the management of genomic programmes. Nat Rev Genet. 2007;8(1):9–22.

41. Li G, Margueron R, Ku M, Chambon P, Bernstein BE, Reinberg D. Jarid2 and PRC2, partners in regulating gene expression. Genes Dev. 2010;24(4):368–80.

42. Baluchamy S, Rajabi HN, Thimmapaya R, Navaraj A, Thimmapaya B. Repression of c-Myc and inhibition of G1 exit in cells conditionally overexpressing p300 that is not dependent on its histone acetyltransferase activity. Proc Natl Acad Sci USA 2003;100(16):9524–9.

43. Chen W, Jia W, Wang K, Si X, Zhu S, Duan T, Kang J. Distinct roles for CBP and p300 on the RA-mediated expression of the meiosis commitment gene Stra8 in mouse embryonic stem cells. PLoS One 2013;8(6):e66076.

44. D'Amour KA, Agulnick AD, Eliazer S, Kelly OG, Kroon E, Baetge EE. Efficient differentiation of human embryonic stem cells to definitive endoderm. Nat Biotechnol. 2005;23(12):1534–41.

45. Sumi T, Tsuneyoshi N, Nakatsuji N, Suemori H. Defining early lineage specification of human embryonic stem cells by the orchestrated balance of canonical Wnt/beta-catenin, Activin/Nodal and BMP signaling. Development 2008;135(17):2969–79.

46. Teo AK, Ali Y, Wong KY, Chipperfield H, Sadasivam A, Poobalan Y, Tan EK, Wang ST, Abraham S, Tsuneyoshi N, Stanton LW, Dunn NR. Activin and BMP4 synergistically promote formation of definitive endoderm in human embryonic stem cells. Stem Cells 2012;30(4):631–42.

47. Cho YM, Lim JM, Yoo DH, Kim JH, Chung SS, Park SG, Kim TH, Oh SK, Choi YM, Moon SY, Park KS, Lee HK. Betacellulin and nicotinamide sustain PDX1 expression and induce pancreatic beta-cell differentiation in human embryonic stem cells. Biochem Biophys Res Commun. 2008;366(1):129–34.

48. Rezania A, Bruin JE, Arora P, Rubin A, Batushansky I, Asadi A, O'Dwyer S, Quiskamp N, Mojibian M, Albrecht T, Yang YH, Johnson JD, Kieffer TJ. Reversal of diabetes with insulin-producing cells derived in vitro from human pluripotent stem cells. Nat Biotechnol. 2014;32(11):1121–33.